

Binary dynamics from Einstein-Maxwell theory at second post-Newtonian order using effective field theory

Pawan Kumar Gupta*

*Institute for Gravitational and Subatomic Physics (GRASP),
Department of Physics, Utrecht University, Princetonplein 1, 3584 CC Utrecht, The Netherlands, EU and
Nikhef, Science Park, 1098 XG Amsterdam, The Netherlands, EU*

The detection of gravitational waves from binary black holes sources has opened the possibility to search for electric charges and “dark” charges on black holes, the latter being candidates for dark matter. This requires theoretical predictions about the effect of charges on the inspiral of binary black holes in order to place constraint on charges. The effects of these charges on the inspiral of binary black holes can be described using Einstein-Maxwell theory. They have previously been derived up to first post-Newtonian (1PN) order, and the results were recently used to place bounds on the charge-to-mass ratio on black holes. Here we use the effective field theory approach with a metric parameterization based on a temporal Kaluza-Klein decomposition with non-relativistic gravitational fields to arrive at the Lagrangian for binary motion under the influence of charges up to 2PN order.

* p.gupta@nikhef.nl

I. INTRODUCTION

To date, the Advanced LIGO [1] and Advanced Virgo [2] gravitational wave (GW) detectors have discovered nearly 90 candidate coalescing binary black holes signals [3–7]. This has opened up avenues to test various physical scenarios, in particular the possibility that binary black holes carry electric charges, or dark charges associated with dark matter candidates [8]. Signals from binary black holes consists of three phases: inspiral, merger, and ringdown. Charges affect the ringdown physics [9–14], and in [15], an analysis of quasi-normal modes was performed on GW150914, leading to 90% upper bounds on the charge-to-mass ratio of the remnant black hole of $|q/m| < 0.33$. Here we focus on the inspiral part of the signal, which can be described analytically through the post-Newtonian (PN) approximation [16, 17]. When charges are introduced, the appropriate model is Einstein-Maxwell theory, where the Lagrangian for binary motion was previously calculated up to first PN (1PN) order in [18, 19] (where the latter also included a dilaton). The results were subsequently used to constrain charges on coalescing binary black holes using gravitational wave signals from the second Gravitational Wave Transient Catalog (GWTC-2); in [8], $1\text{-}\sigma$ constraints of $|q/m| \leq 0.2 - 0.3$ were placed.

Considering further improvements in detector sensitivities, and in particular the planned next-generation GW observatories Einstein Telescope [20, 21], Cosmic Explorer [22], and LISA [23–25], more accurate theoretical predictions are in order. In this work we calculate the Lagrangian for two inspiraling bodies with charges included to 2PN order, using the effective field theory (EFT) approach.

The EFT approach was first suggested by Goldberger and Rothstein to solve the binary inspiral problem in an alternative way [26, 27]. It efficiently uses standard tools from quantum field theory such as Feynman diagrams and dimensional regularization, but now applied to the classical two-body problem in GR. Currently the framework has been used up to 5PN order [28–30], with inclusion of spin-orbit and spin-spin effects to 3PN order [31–34].

A novel method within the EFT approach was suggested by Kol and Smolkin (KS), who used a temporal Kaluza-Klein parameterization of the metric which improved the computational efficiency [35]. This non-relativistic parameterization defines a set of new non-relativistic gravitational (NRG) fields. As we shall see, when charges are included this leads to a clear coupling hierarchy between mass and charge, so that the technique is particular suited to our problem. More generally, the KS parameterization has been shown to reduce the complexity involved in calculating the Einstein-Infeld-Hoffmann (1PN) Lagrangian [35] and the 2PN Lagrangian [36]. Similar simplifications were observed in the calculation of the various contributions to the spin-spin potential [37–40] as well as to the spin-orbit potential [41–43].

In this paper, we calculate the Lagrangian for Einstein-Maxwell action up to 2PN order using EFT with NRG fields. We recover the Coulomb potential using a single diagram then reproduce the 1PN order Lagrangian which requires only 6 diagrams to be computed and agrees with the known result [18, 19]. At 1PN order, we encounter a 1-loop integral which we solve using a master formula Eq. A7. At 2 PN order, we find there are 20 diagrams which have 1-loop and 26 diagrams which have 2-loop contributing. At 2-loops, We encounter that some of the integral going to infinity, which we take care of by using standard dimensional regularisation technique. We demonstrate how the EFT with NRG fields can be used to efficiently compute conservative binary dynamics with charge at high precision in the PN expansion.

This paper is organized as follows. In Sec. II A we expand the non-charged point particle action up to 2PN order and derive the Feynman rules for NRG fields couplings to worldlines, and in Sec. II B we do the same with charge included. In Sec. II C we write the Einstein-Hilbert action up to 2PN order with a gauge fixing term and derive its propagators and self-gravitational vertices; in Sec. II D we again introduce charges. In Sec. II E, we explain the terms that will contribute to 2PN order and relevant Feynman diagrams. Next, in Sec. III, we compute the Coulomb potential using the Feynman rules we have obtained. In Sec. IV, we calculate the relevant 1PN order Feynman diagram, and summarize the Lagrangian. In Sec. V we calculate the 2PN order Feynman diagrams, and summarize the Lagrangian. In Sec. VI we show the Lagrangian up to 2PN order and discuss various aspects of it. A summary and conclusions are given in Sec. VII, along with future directions. Appendix A contains a short compilation of useful formulas.

Throughout this paper we write $\int_k = \int \frac{d^3\vec{k}}{(2\pi)^3}$. The speed of light c is set to 1, except in cases where we make explicit the post-Newtonian counting in powers of $1/c^2$. Greek letters μ, ν, \dots denote four-dimensional spacetime coordinate indices, while lowercase Latin letters i, j, k, \dots are spatial coordinate indices. Our metric signature is $\eta_{ab} = \text{diag}(-1,$

+1, +1, +1). Our convention for the Riemann tensor is

$$R^\mu{}_{\nu\alpha\beta} = \Gamma^\mu{}_{\nu\beta,\alpha} - \Gamma^\mu{}_{\nu\alpha,\beta} + \Gamma^\rho{}_{\nu\beta}\Gamma^\mu{}_{\rho\alpha} - \Gamma^\rho{}_{\nu\alpha}\Gamma^\mu{}_{\rho\beta}, \quad (1)$$

where $\Gamma^\mu{}_{\nu\beta}$ are the Christoffel symbols, and a comma denotes a partial derivative.

II. EINSTEIN-MAXWELL THEORY

In this section we briefly review the action for Einstein-Maxwell theory for inspiraling binary black holes with charge. We work within a non-relativistic form of the Kaluza-Klein ansatz for the metric, which has a set of non-relativistic gravitational (NRG) fields. We write the point particle action in terms of this metric and expand it up to second 2PN order. From this we extract the worldline couplings of the NRG fields. Similarly, we extract the worldline coupling of electromagnetic (EM) fields using the charged particle action up to 2PN order. In order to find out how the NRG fields interact with the worldline vertex, we derive the propagators for NRG fields using the Einstein-Hilbert action with harmonic gauge up to 2PN order. We write the action of the EM fields in the Feynman gauge and derive their propagator. We also derive Feynman rules for 3 EM fields interacting together, called the 3-point vertex, and 4 EM fields interacting together called the 4-point vertex at 2PN order. Finally, we discuss PN order counting rules for Feynman diagrams.

The inspiral dynamics of binary black holes with charges is described by Einstein-Maxwell theory, which has following action:

$$\mathcal{S} = \mathcal{S}_{pp} + \mathcal{S}_q + \mathcal{S}_g + \mathcal{S}_{em}, \quad (2)$$

where \mathcal{S}_{pp} is the point particle action, which we describe in the following subsection. \mathcal{S}_q is the charged particle action,

$$\mathcal{S}_q = \int dt q v^\mu A_\mu = - \int dt q A_0 + \int dt q v^i A_i, \quad (3)$$

where q is the charge, v^μ the four-velocity, and A^μ the four-vector potential. \mathcal{S}_g is the Einstein-Hilbert action with a harmonic gauge term:

$$\mathcal{S}_g = \mathcal{S}_{EH} + \mathcal{S}_{GF,g} = \frac{1}{16\pi} \int d^4x \sqrt{-g} R - \frac{1}{32\pi G} \int d^4x \sqrt{-g} g_{\mu\nu} \Gamma^\mu \Gamma^\nu. \quad (4)$$

\mathcal{S}_{em} is the electromagnetic action in curved spacetime with Feynman gauge,

$$\mathcal{S}_{em} = \mathcal{S}_M + \mathcal{S}_{GF,em} = \frac{-1}{16\pi} \int d^4x \sqrt{-g} (F^2 + 2(\partial_\mu A^\mu)^2), \quad (5)$$

where $F_{\mu\nu} = \nabla_\mu A_\nu - \nabla_\nu A_\mu$.

We use the metric in a non-relativistic form according to the Kaluza-Klein (KK) ansatz,

$$d\tau^2 = g_{\mu\nu} dx^\mu dx^\nu \equiv -e^{2\phi} (dt - \mathcal{A}_i dx^i)^2 + e^{-2\phi} \gamma_{ij} dx^i dx^j, \quad (6)$$

where $\phi, \mathcal{A}_i, \gamma_{ij} \equiv \delta_{ij} + \sigma_{ij}$ are a set of NRG fields. We can write the matrix form of the metric in terms of the NRG fields as

$$g_{\mu\nu} = \begin{pmatrix} -e^{2\phi} & e^{2\phi} \mathcal{A}_j \\ e^{2\phi} \mathcal{A}_i & e^{-2\phi} \gamma_{ij} - e^{2\phi} \mathcal{A}_i \mathcal{A}_j \end{pmatrix}. \quad (7)$$

There is a physical meaning associated with the NRG fields: ϕ can be identified with the Newtonian potential, \mathcal{A}_i is the gravito-magnetic potential, and σ_{ij} is the 3-metric tensor [35, 44]. The leading PN order of NRG fields ϕ, \mathcal{A}_i and σ_{ij} are $\mathcal{O}(1/c^2)$, $\mathcal{O}(1/c^3)$, and $\mathcal{O}(1/c^4)$ respectively.

A. Point Particle Action

In the EFT approach, the binary black holes are treated as point particles on worldlines described by the action

$$\mathcal{S}_{pp} = - \sum_{i=1}^2 m_i \int d\tau_i = - \sum_{i=1}^2 \int dt m_i \sqrt{-g_{\mu\nu} v_i^\mu v_i^\nu}, \quad (8)$$

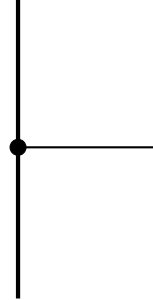
where m_i , $i = 1, 2$ are the individual point particle masses. Here it is convenient to parameterize the worldline using coordinate time t . The point particle action of Eq. (8) contains two terms coming from each of the two point particles, which are the same except for the labeling $i = 1, 2$. We consider the action without this label and expand it using the KK metric of Eq. (6),

$$\mathcal{S}_{pp} = - \int dt m e^\phi \sqrt{-(1 - 2\mathcal{A}_i v^i) + (1 - 4\phi + 8\phi^2)(\delta_{ij} + \sigma_{ij})v^i v^j}. \quad (9)$$

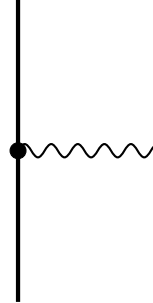
We can expand this action up to 2PN order,

$$\mathcal{S}_{pp} = -m \int dt \left(1 - \frac{1}{2}v^2 + \phi - \mathcal{A}_i v^i - \frac{1}{8}v^4 + \frac{3}{2}\phi v^2 + \frac{1}{2}\phi^2 - \frac{1}{2}v^i v^j \sigma_{ij} - \frac{1}{16}v^6 \right), \quad (10)$$

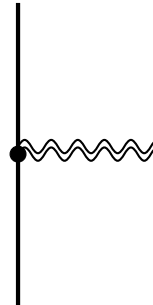
where we have used the leading PN order of the NRG fields to find the 2PN order terms. We extract the vertex for the NRG fields coupling to the worldline mass up to 2PN order:



$$= -m \int dt \phi \left\{ 1 + \frac{3}{2}v^2 \right\}, \quad (11)$$

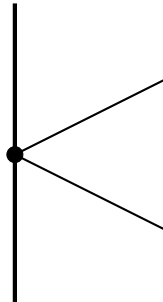


$$= m \int dt \mathcal{A}_i v^i, \quad (12)$$



$$= \frac{m}{2} \int dt \sigma_{ij} v^i v^j \quad (13)$$

where the heavy solid lines represent the worldlines and the black blobs represent the particle mass on the worldline. Similarly, we extract the two scalar NRG field exchange,



$$= -\frac{1}{2}m \int dt \phi^2 \quad (14)$$

These are the only possible NRG fields coupling with worldline particle up to 2PN order. Using a similar procedure one can extend this to higher PN order couplings of NRG fields.

B. Charged Particle Action

The contribution to the worldline action due to charge is

$$\mathcal{S}_q = \int dt q v^\mu A_\mu = - \int dt q A_0 + \int dt q v^i A_i. \quad (15)$$

We expand this action using the KK metric Eq. (6):

$$\mathcal{S}_q = - \int dt q A_0 e^{2\phi} + \int dt q v^i A^j e^{-2\phi} (\sigma_{ij} + \delta_{ij}) + \int dt q A^0 v^i e^{2\phi} \mathcal{A}_i + \int dt q A^i e^{2\phi} \mathcal{A}_i. \quad (16)$$

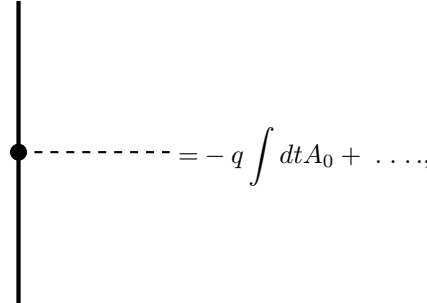
The leading PN order for the electromagnetic fields A_0 and A_i are $\mathcal{O}(1/c^0)$ and $\mathcal{O}(1/c^1)$, respectively [19]. We can expand the action up to 2PN order,

$$\mathcal{S}_q = - \int dt q A_0 (1 + 2\phi + 2\phi^2) + \int dt q v^i A^i (1 - 2\phi) + \int dt q A^0 v^i \mathcal{A}_i + \int dt q A^i \mathcal{A}_i. \quad (17)$$

The 1PN order term of Eq. (17) is

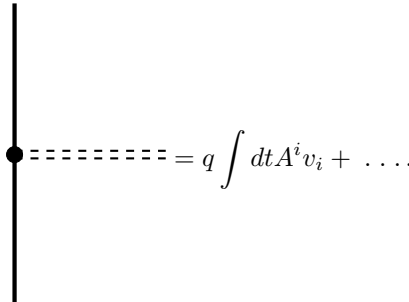
$$\mathcal{S}_q = \int dt q v^\mu A_\mu = - \int dt q A_0 - \int dt q A_0 2\phi + \int dt q v^i A^i. \quad (18)$$

We find the scalar electromagnetic field worldline vertex to be



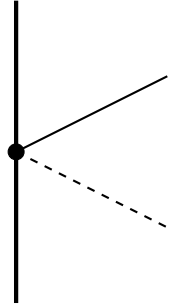
$$= -q \int dt A_0 + \dots, \quad (19)$$

and the vector electromagnetic field worldline vertex to be



$$= q \int dt A^i v_i + \dots \quad (20)$$

We also find the scalar NRG field and scalar electromagnetic field worldline vertex at 1PN order,

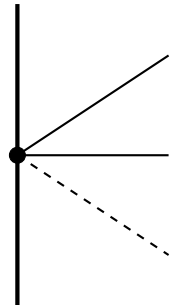


$$= -2q \int dt A_0 \phi + \dots \quad (21)$$

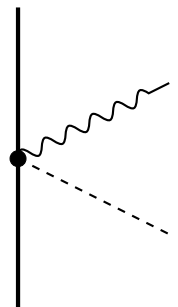
The 2PN order term of Eq. (17) is

$$\mathcal{S}_q = - \int dt \, q A_0 2\phi^2 + \int dt \, q v^i A^i 2\phi + \int dt \, q A^0 v^i \mathcal{A}_i + \int dt \, q A^i \mathcal{A}_i. \quad (22)$$

The worldline vertex corresponding to 2PN is

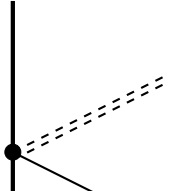


$$= -2q \int dt A_0 \phi^2 + \dots \quad (23)$$

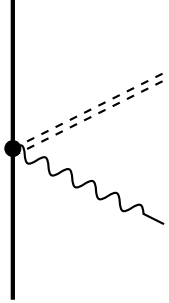


$$= q \int dt A^0 \mathcal{A}_i v^i + \dots \quad (24)$$

(25)



$$= 2q \int dt v^i A_i \phi \dots \quad (26)$$



$$= q \int dt \mathcal{A}^i A_i \dots \quad (27)$$

We find the worldline vertex with NRG fields and EM fields together.

C. Einstein-Hilbert Action

We consider the gravitational action to be the Einstein-Hilbert action together with a harmonic gauge fixing term:

$$\mathcal{S}_g = \mathcal{S}_{EH} + \mathcal{S}_{GF,g} = \frac{1}{16\pi} \int d^4x \sqrt{-g} R - \frac{1}{32\pi G} \int d^4x \sqrt{-g} g_{\mu\nu} \Gamma^\mu \Gamma^\nu, \quad (28)$$

where $\Gamma^\mu \equiv \Gamma_{\rho\sigma}^\mu g^{\rho\sigma}$. Using the KK metric of Eq. (6), \mathcal{S}_g , the gravitational action can be written as [35]

$$\mathcal{S}_g = \frac{1}{16\pi G} \int dt d^3x \sqrt{\gamma} \left(R[\gamma] - 2\partial_i \phi \partial^i \phi + \frac{1}{4} e^{4\phi} \mathcal{F}^2 \right), \quad (29)$$

with $\partial_i \partial^i \phi = \gamma^{ij} \partial_i \phi \partial_j \phi$, and where we have defined the analog of the field strength tensor, F , but in terms of the KK gravitomagnetic tensor, \mathcal{A}_i , such that $\mathcal{F}_{ij} = \partial_i \mathcal{A}_j - \partial_j \mathcal{A}_i$.

Using the gravitational action of Eq. (29) we find the NRG field propagators: [37],

$$\text{—————} = \langle \phi(x_1) \phi(x_2) \rangle = 4\pi G \delta(t_1 - t_2) \int_k \frac{e^{i\vec{k} \cdot \vec{r}}}{\vec{k}^2}, \quad (30)$$

$$\text{~~~~~} = \langle \mathcal{A}_i(x_1) \mathcal{A}_j(x_2) \rangle = -16\pi G \delta(t_1 - t_2) \int_k \frac{e^{i\vec{k} \cdot \vec{r}}}{\vec{k}^2} \delta_{ij}, \quad (31)$$

$$\text{~~~~~} = \langle \sigma_{ij}(x_1) \sigma_{kl}(x_2) \rangle = 32\pi G P_{ij;kl} \delta(t_1 - t_2) \int_k \frac{e^{i\vec{k} \cdot \vec{r}}}{\vec{k}^2}, \quad (32)$$

where $P_{ij;kl} \equiv \frac{1}{2} (\delta_{ik} \delta_{jl} + \delta_{il} \delta_{jk} - 2\delta_{ij} \delta_{kl})$, $\vec{r} = |\vec{x}_1 - \vec{x}_2|$, and the propagator is instantaneous [45],

$$\int \frac{dk_0}{2\pi} e^{-ik_0 t} \int \frac{d^3 \vec{k}}{(2\pi)^3} \frac{e^{i\vec{k} \cdot \vec{x}}}{\vec{k}^2} = \delta(t) \int \frac{d^3 \vec{k}}{(2\pi)^3} \frac{e^{i\vec{k} \cdot \vec{x}}}{\vec{k}^2} \quad (33)$$

where we have used the scaling of the orbital modes, $k_0 = v/r$ and $|\vec{k}| = 1/r$.

We also get corrections to the instantaneous nature of the non-relativistic potential propagators. The Feynman rules for the propagator correction vertices are given by

$$\text{---}\times\text{---} = \frac{1}{2!} \frac{1}{4\pi G} \int d^4x \partial^0 \phi \partial^0 \phi \quad (34)$$

where the crosses represent the self-gravitational quadratic vertices, which contain two time derivatives. Notice that the usual procedure is to drop the factors $1/i!$ for i identical lines on a vertex and multiply the diagram by $1/(\text{symmetry factor})$ instead. From now on we present the vertex rules with the $1/i!$ dropped:

$$\text{---}\times\text{---} = \frac{1}{4\pi G} \int d^4x \partial^0 \phi \partial^0 \phi \quad (35)$$

D. Electromagnetic action

We consider the electromagnetic action in curved spacetime a Feynman gauge fixing term:

$$\mathcal{S}_{em} = \mathcal{S}_M + \mathcal{S}_{GF,em} = \frac{-1}{16\pi} \int d^4x \sqrt{-g} (F^2 + 2(\partial_\mu A^\mu)^2), \quad (36)$$

where $F_{\mu\nu} = \nabla_\mu A_\nu - \nabla_\nu A_\mu = \partial_\mu A_\nu - \partial_\nu A_\mu$. Because of expanding the covariant derivative into partial derivatives and Christoffel symbols, the Christoffel symbols cancel out and there are only partial derivatives left.

We can further expand the action in Eq. (36) using the KK metric of Eq. (6) up to 2PN order:

$$\begin{aligned} \mathcal{S}_q = \frac{-1}{16\pi} \int d^4x & \left(-2(\partial^i A^0)^2 + (2(\partial^i A^k \partial^i A^k) + 2\partial^0 A^0 \partial^0 A^0 + 4\phi(\partial^i A^0)^2) \right. \\ & - 2(\partial^0 A^i)^2 + 8\phi \partial^0 A^0 \partial^0 A^0 - 4\mathcal{A}_j \partial^0 A^0 \partial^j A^0 - 8\phi(\partial^i A^k \partial^i A^k) - 2\sigma_{ij}(\partial^j A^0)(\partial^i A^0) \\ & \left. + 4\mathcal{A}_j(\partial^i A^j)(\partial^i A^0) - 2\phi(2(\partial^i A^k \partial^i A^k) + 2\partial^0 A^0 \partial^0 A^0) - 2(\partial^i A^0)^2 \left(\frac{1}{2}\sigma_i^i + 2\phi^2 \right) \right) \end{aligned} \quad (37)$$

This action agrees with the one resulting from a calculation with the EFTofPNG package [46]. We find the electromagnetic field propagators from the first and second terms of Eq. (37) to be

$$\text{-----} = \langle A^0(x_1) A^0(x_2) \rangle = -4\pi \delta(t_1 - t_2) \int_k \frac{e^{i\vec{k}\cdot\vec{r}}}{\vec{k}^2}, \quad (38)$$

$$\text{=====} = \langle A_i(x_1) A_j(x_2) \rangle = 4\pi \delta(t_1 - t_2) \int_k \frac{e^{i\vec{k}\cdot\vec{r}}}{\vec{k}^2} \delta_{ij}, \quad (39)$$

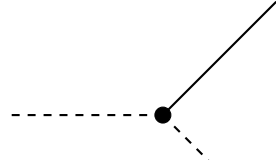
We get corrections to the instantaneous nature of the non-relativistic potential propagators. The Feynman rules for the propagator correction vertices come from the third and fifth terms of Eq. (37),

$$\text{-----}\times\text{-----} = \frac{-1}{4\pi} \int d^4x \partial^0 A^0 \partial^0 A^0, \quad (40)$$

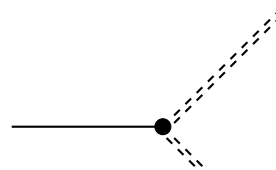
$$\text{=====}\times\text{=====} = \frac{1}{4\pi} \int d^4x \partial^0 A^i \partial^0 A^i, \quad (41)$$

where the crosses represent the self-electromagnetic quadratic vertices, which contain two time derivatives.

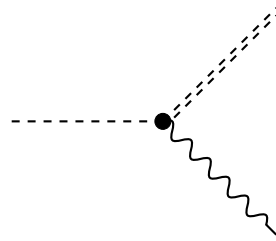
We extract the three-point self-interacting vertex from Eq. (37),



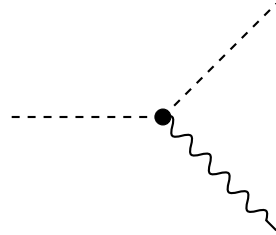
$$= \frac{-1}{8\pi} \int d^4x \left(4\phi(\partial^i A^0)^2 + 4\phi\partial^0 A^0\partial^0 A^0 \right), \quad (42)$$



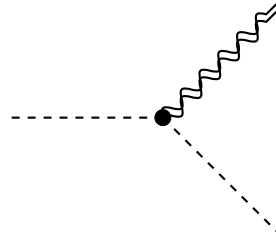
$$= \frac{-1}{8\pi} \int d^4x \left(-12 \right) \phi(\partial^i A^k \partial^i A^k), \quad (43)$$



$$= \frac{-1}{16\pi} \int d^4x \left(4\mathcal{A}_j(\partial^i A^j)(\partial^i A^0) \right), \quad (44)$$

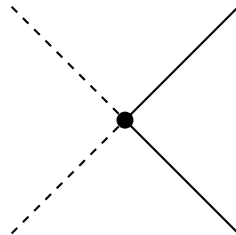


$$= \frac{-1}{8\pi} \int d^4x \left(-4 \right) \mathcal{A}_j \partial^0 A^0 \partial^j A^0, \quad (45)$$



$$= \frac{-1}{8\pi} \int d^4x \left(-2 \right) \sigma_{ij}(\partial^j A^0)(\partial^i A^0) - 2(\partial^i A^0)^2 \sigma_i^i. \quad (46)$$

We extract a four-point vertex from the last term of Eq. (37),



$$= \frac{-1}{4\pi} \int d^4x \left(-4 \right) (\partial^i A^0)^2 \phi^2 \quad (47)$$

There are two kinds of two identical lines on the vertex, and we have dropped the factors $1/2!$ and $1/2!$.

0PN	1PN	2PN	3PN
q^2	$q^2 v^2$	$q^2 v^4$	$q^2 v^6$
	Gq^2	$Gq^2 v^2$	$Gq^2 v^4$
		$G^2 q^2$	$G^2 q^2 v^2$
		Gq^4	$Gq^4 v^2$

TABLE I: This table shows the order of the terms that contribute at given PN orders.

E. Power counting and Feynman diagrams

For a bound state, the virial theorem relates the orbital velocity v , Newton's constant G and charge q via $v^2 \sim Gm/r \sim q^2/r$. Keeping this in mind, we count powers of G , q^2 , and v^2 separately to get the corresponding PN order. From Table I we can see that the diagram responsible for the Coulomb potential scales as $\mathcal{O}(q^2)$. We also compute 1PN order diagrams which scale as $\mathcal{O}(q^2 v^2)$ and $\mathcal{O}(Gq^2)$. For the 2PN potential calculation, we need to include all diagrams which scale as $\mathcal{O}(q^2 v^4)$, $\mathcal{O}(Gq^2 v^2)$, $\mathcal{O}(G^2 q^2)$, and $\mathcal{O}(Gq^4)$. Diagrams without charge interaction have already been computed; see [36].

We first generate all the relevant Feynman diagram topologies up to G^3 following the rules of counting powers of G : When there are n gravitons attached to a worldline, it has a power of $G^{n/2}$, and each n -graviton self-interaction vertex has a power of $G^{(n/2-1)}$ [36]. After counting powers of G , we need to count the powers of velocity for each Feynman diagram. The rules for counting powers of v^2 for NRG fields ϕ , \mathcal{A}_i , and σ_{ij} coupling to the worldlines are $\mathcal{O}(v^0)$, $\mathcal{O}(v^1)$, and $\mathcal{O}(v^2)$ respectively. For the EM fields, the couplings of A_0 and A_i are $\mathcal{O}(v^0)$ and $\mathcal{O}(v^1)$ respectively. We can also have 2 or 3 EM fields couplings to worldlines with various order in velocity that we can see from Sec. II B. Time derivatives can arise from either purely gravitational interaction vertices or electromagnetic interaction vertices, where each time derivative insertion counts as $\mathcal{O}(v^2)$. Finally, we perform counting for q^2 ; all the contributions of q^2 come from the fields couplings with the worldlines Sec. II B.

We generate all relevant diagram topologies and populate the diagrams with the three NRG fields ϕ , \mathcal{A}_i , and σ_{ij} and EM fields A_0 and A_i in all allowed combinations. We then count the factors of v which result from the gravitational fields and electromagnetic fields coupling to the worldline, and any time derivatives acting on internal vertices. We count the factors of q which result from fields coupling with worldlines. After counting power of G , v^2 and q^2 , we can identify the relevant diagrams at a given PN order. The diagrams relevant at 0PN order which result from this procedure are shown in Fig. 1, the ones at 1PN order in Fig. 2, and the ones at 2PN order in Figs. 3, 4, 5, and 6. We have ignored diagrams with gravitational loops since they include quantum effects [47].

III. COULOMB POTENTIAL

In this section, we compute the Coulomb potential term using the relevant Feynman diagram.

We start with diagram 1(a) in Fig. 1(a). To compute this diagram, we need two copies of the worldline coupling with the EM scalar field of Eq. (19) and the propagator for the scalar EM field in Eq. (38):

$$\begin{aligned}
\text{Diagram 1(a)} &= q_1 q_2 \int dt_1 \int dt_2 \langle A_0(x_1, t_1) A_0(x_2, t_2) \rangle \\
&= q_1 q_2 \int dt_1 \int dt_2 (-4\pi) \delta(t_1 - t_2) \int_k \frac{e^{i\vec{k} \cdot \vec{r}}}{k^2} \\
&= -4\pi q_1 q_2 \int dt \frac{1}{4\pi r} = \int dt \frac{-q_1 q_2}{r}.
\end{aligned} \tag{48}$$

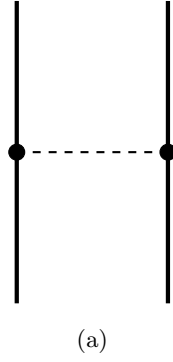


FIG. 1: Diagram (a) shows the Coulomb interaction at $\mathcal{O}(q^2)$

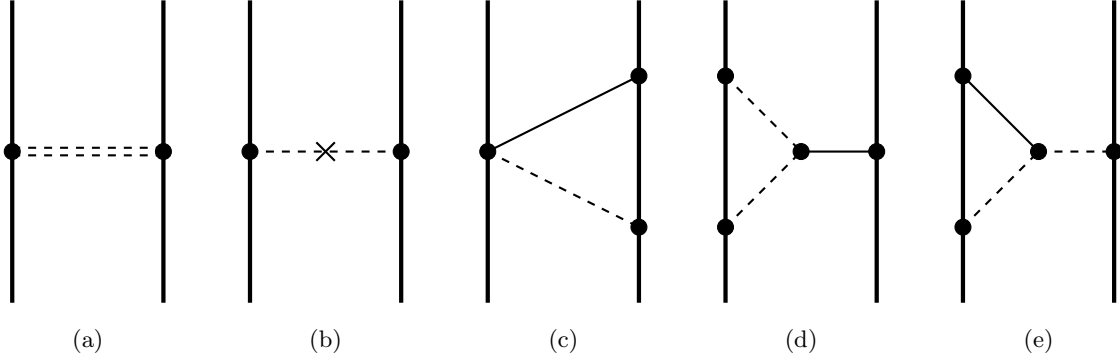


FIG. 2: Diagrams (b) and (c) are 1PN corrections at $\mathcal{O}(q^2 v^2)$, and the rest of the diagrams are also 1PN corrections at $\mathcal{O}(Gq^2)$

After performing the Fourier integral using identity (A2) we get the Coulomb potential term.

IV. 1 PN ORDER POTENTIAL

In this section we compute the 1PN Feynman diagrams, which include $\mathcal{O}(Gq^2)$ and $\mathcal{O}(v^2 q^2)$ contributions. We explicitly show how to compute the diagrams 2(c) in Fig. 2, which have a time derivative, and the diagrams 2(e) in Fig. 2 which have one loop integral. The symmetry factors of the diagram are computed as described in [36]; another way to compute them is using Wick's theorem and considering no time ordering. We specify the symmetry factor for a diagram when it is not 1. Finally, we get the 1PN Lagrangian from adding the contributions from all the 1PN diagrams.

A. $q^2 v^2$ order diagrams

Diagram 2(a) in Fig. 2 is computed using two copies of worldline couplings with the vector EM field in Eq. (20), the propagator for the vector EM field in Eq. (39), and the formula in Eq. A2:

$$\begin{aligned}
 \text{Diagram 2(a)} &= \int dt_1 q_1 v_1^i \int dt_2 q_2 v_2^j \langle A^i(x_1) A^j(x_2) \rangle \\
 &= q_1 q_2 \int dt_1 v_1^i \int dt_2 v_2^j 4\pi \delta(t_1 - t_2) \int_k \frac{e^{i\vec{k} \cdot \vec{r}}}{\vec{k}^2} \delta_{ij} \\
 &= \int dt \frac{q_1 q_2}{r} (\vec{v}_1 \cdot \vec{v}_2).
 \end{aligned} \tag{49}$$

Diagram 2(b) in Fig. 2 contains a time derivative. It is computed as

$$\text{Diagram 2(b)} = \int dt_1 q_1 A_0(x_1, t_1) \int dt_2 q_2 A_0(x_2, t_2) \frac{1}{4\pi} \int d^4x \partial^0 A^0 \partial^0 A^0, \quad (50)$$

where we have used Eq. (19) for the world line couplings and Eq. (40) for time derivative terms. We further simplify the integral using the scalar EM field propagator in Eq. (38):

$$\text{Diagram 2(b)} = -4\pi q_1 q_2 \int d^4x \int dt_1 \int dt_2 \partial^t \delta(t_1 - t) \partial^t \delta(t_1 - t) \int_{k_1} \frac{e^{\vec{k}_1 \cdot (x_1 - x)}}{k_1^2} \int_{k_2} \frac{e^{\vec{k}_2 \cdot (x_2 - x)}}{k_2^2}. \quad (51)$$

Integrating over d^3x gives a delta function in momentum:

$$\text{Diagram 2(b)} = -4\pi q_1 q_2 \int dt \int dt_1 \int dt_2 \partial^t \delta(t_1 - t) \partial^t \delta(t_1 - t) \int_{k_1} \frac{e^{\vec{k}_1 \cdot x_1}}{k_1^2} \int_{k_2} \frac{e^{\vec{k}_2 \cdot x_2}}{k_2^2} (2\pi)^3 \delta^3(k_1 + k_2). \quad (52)$$

After performing the momentum integral over the delta function and flipping the time derivative using the identity (A1),

$$\text{Diagram 2(b)} = -4\pi q_1 q_2 \int dt \int dt_1 \int dt_2 \partial^{t_1} \delta(t_1 - t) \partial^{t_2} \delta(t_1 - t) \int_{k_1} \frac{e^{\vec{k}_1 \cdot (x_1(t_1) - x_2(t_2))}}{k_1^4}. \quad (53)$$

The integration is further performed using the tensor Fourier identity A3:

$$\text{Diagram 2(b)} = - \int dt \frac{q_1 q_2}{2r} \left(\vec{v}_1 \cdot \vec{v}_2 - \frac{(\vec{v}_1 \cdot \vec{r})(\vec{v}_2 \cdot \vec{r})}{r^2} \right). \quad (54)$$

B. Gq^2 order diagrams

Diagram 2(c) in Fig. 2 is computed using Eqs. (11), (19), and (21) for worldline couplings, and Eqs. (11), (38) for the propagator, together with the identity (A2):

$$\text{Diagram 2(c)} = \int dt_1 \frac{2Gm_2 q_1 q_2}{r^2}. \quad (55)$$

Diagram 2(d) in Fig. 2 is difficult to compute; let us go through it in steps. First,

$$\text{Diagram 2(d)} = \int dt_1 q_1 A_0(x_1) \int dt_2 q_1 A_0(x_1) \int dt_3 (-m_2) \phi(x_2) \frac{-1}{8\pi} \int d^4x 4\phi \partial^i A^0 \partial^j A^0 \delta_{ij}, \quad (56)$$

where we used the 3-point vertex from Eq. (43). We then perform the integration over d^3x and time, which yields

$$\text{Diagram 2(d)} = (4\pi)^2 Gm_2 q_1^2 \int dt \int_{k_2} \int_{k_3} \frac{e^{i\vec{k}_3 \cdot (\vec{x}_2 - \vec{x}_1)}}{(\vec{k}_2 + \vec{k}_3)^2} \frac{(k_2^i + k_3^i) k_2^j}{k_2^2 k_3^2} \delta_{ij}. \quad (57)$$

This integral is solved the using 1-loop master integral (A7),

$$\text{Diagram 2(d)} = - \int dt \frac{Gm_2 q_1^2}{r^2}. \quad (58)$$

The symmetry factor of this diagram is $\frac{1}{2}$, which needs to be multiplied,

$$\text{Diagram 2(d)} = - \int dt \frac{Gm_2 q_1^2}{2r^2}. \quad (59)$$

We compute the diagram 2(e) similarly,

$$\begin{aligned} \text{Diagram 2(e)} &= - \int dt_1 q_1 A_0(x_1) 2\phi(x_1) \int dt_2 (-q_2) A_0(x_2) \int dt_3 (-m_2) \phi(x_2, t_3) \\ &= - \int dt_1 \frac{Gm_2 q_1 q_2}{r^2}. \end{aligned} \quad (60)$$

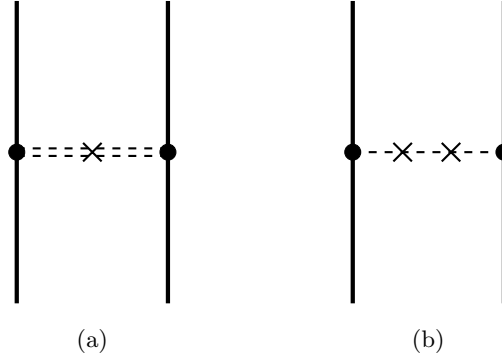


FIG. 3: Diagrams that have $\mathcal{O}(q^2 v^4)$ and time derivatives.

Putting together the contributions from all 1PN diagrams we obtain the Lagrangian

$$\mathcal{L}_{1PN} = \frac{q_1 q_2}{r} (\vec{v}_1 \cdot \vec{v}_2) - \frac{q_1 q_2}{2r} \left(\vec{v}_1 \cdot \vec{v}_2 - \frac{(\vec{v}_1 \cdot \vec{r})(\vec{v}_2 \cdot \vec{r})}{r^2} \right) + \frac{G q_1 q_2}{r^2} (m_2 + m_1) - \frac{G}{2r^2} (m_2 q_1^2 + m_1 q_2^2), \quad (61)$$

and there is a similar contribution from changing $1 \leftrightarrow 2$. This 1PN Lagrangian agrees what was obtained in [18, 19].

V. 2PN ORDER

In this section we compute the 2PN Feynman diagrams. For 2PN diagrams, we can have $\mathcal{O}(q^2 v^4)$, $\mathcal{O}(G q^2 v^2)$, $\mathcal{O}(G q^4)$, and $\mathcal{O}(G^2 q^2)$ diagrams, which are computed in the subsections below. The $\mathcal{O}(q^2 v^4)$ order diagrams involve time derivatives and are computed in the same way as diagram 2(c) in Fig. 2. The $\mathcal{O}(G q^2 v^2)$ order diagrams have 1-loop integrals and a time derivative and are computed similarly to the 1 PN order diagrams. The $\mathcal{O}(G q^4)$ and $\mathcal{O}(G^2 q^2)$ order diagrams have 2 loop integrals which are of three types. The first type consists of factorizable 2-loops integrals which factorize into a product of two 1-loop integrals, such that each 1-loop can be performed separately. These types of integrals are relatively easier to compute. The second type consists of nested 2-loops, or recursively 1-loops, on which a 1-loop is nested in a another loop, so that they should be performed successively, first the nested 1-loop, then the outer 1-loop. The third type consists of irreducible 2-loops, which can be formally reduced, using an integration by parts method [48], to a sum of integrals of the two previous kinds, i.e. to a sum of factorizable and nested two-loops. We specify the symmetry factor for a diagram when is it not 1 and show the results for diagrams with symmetry factor included.

A. $q^2 v^4$ order diagrams

There are only two diagrams of this order. Neither diagram contains any graviton exchange, as shown in Fig. 3. These diagrams have time derivatives and are computed similarly to diagram 1(e):

$$\text{Diagram 3(a)} = \int dt \frac{q_1 q_2}{2r} \left(\vec{v}_1 \cdot \vec{v}_2 - \frac{(\vec{v}_1 \cdot \vec{r})(\vec{v}_2 \cdot \vec{r})}{r^2} \right) (\vec{v}_1 \cdot \vec{v}_2), \quad (62)$$

and

$$\begin{aligned} \text{Diagram 3(b)} = \int dt 2q_1 q_2 & \left(\frac{3(\vec{n} \cdot \vec{v}_1)^2 (\vec{n} \cdot \vec{v}_2)^2}{16r} + \frac{2(\vec{v}_1 \cdot \vec{v}_2)^2 + \vec{v}_1^2 \vec{v}_2^2}{16r} - \frac{4(\vec{n} \cdot \vec{v}_1)(\vec{n} \cdot \vec{v}_2)(\vec{v}_1 \cdot \vec{v}_2)}{16r} \right. \\ & \left. - \frac{(\vec{n} \cdot \vec{v}_1)^2 \vec{v}_2^2 - (\vec{n} \cdot \vec{v}_2)^2 \vec{v}_1^2}{16r} \right). \end{aligned} \quad (63)$$

B. $G q^2 v^2$ order diagrams

We have 20 diagrams at the $G q^2 v^2$ order; out of these, 14 diagrams have 3-point vertex. These are computed similarly to 1PN order diagrams, as these diagrams involves a time derivative and a 3-point vertex. All the diagrams

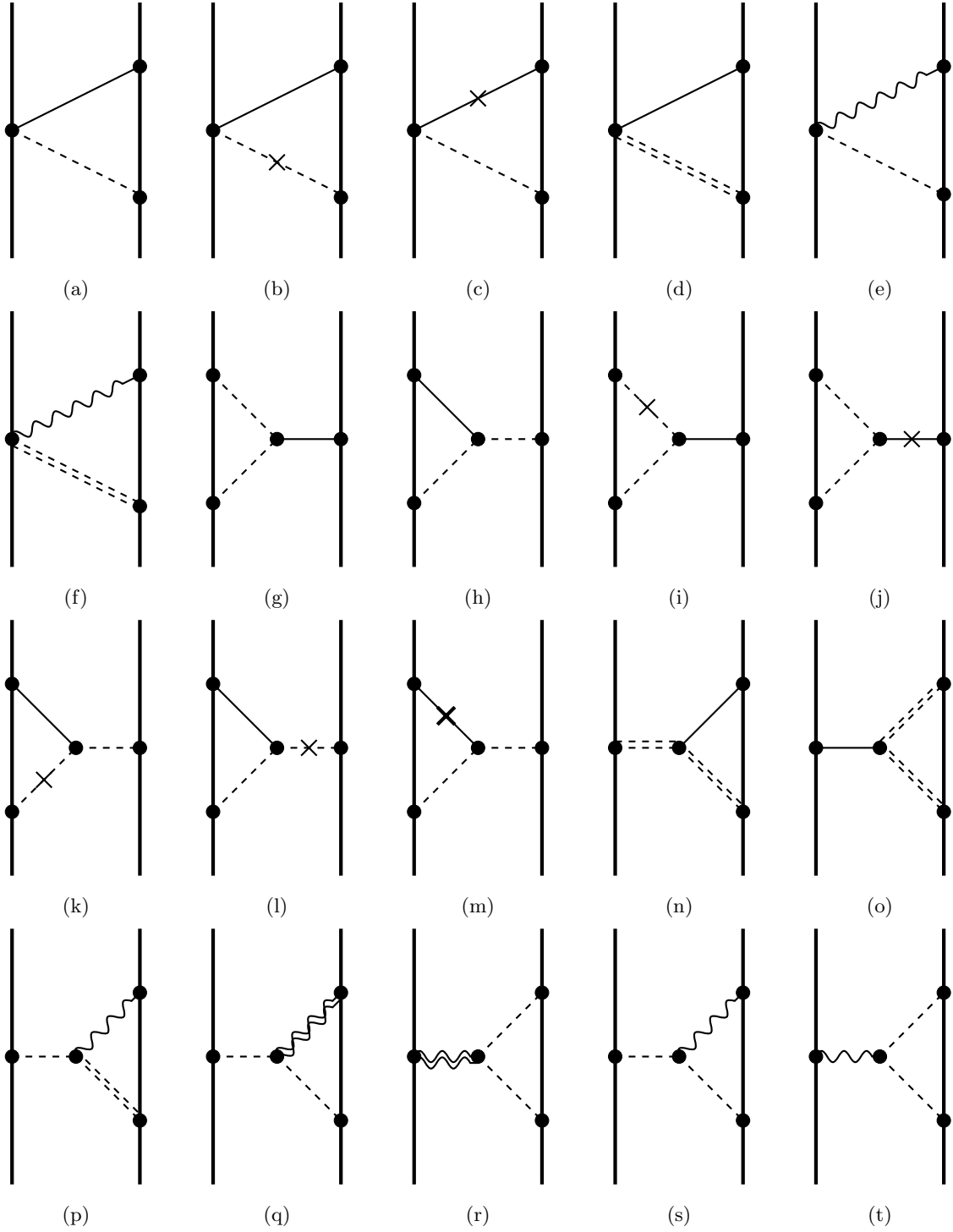


FIG. 4: Diagrams that have $\mathcal{O}(Gq^2v^2)$.

have single graviton exchange. There are diagrams from 1PN order which also contribute at 2PN order, namely 2(c), 2(d), and 2(e). The diagrams 4(g), 4(i), 4(j), 4(o), 4(r), and 4(t) in Fig. 4 have a symmetry factor of $1/2$ while the rest of the diagrams have a symmetry factor of 1.

The diagrams 4(a) to 4(f) in Fig 4 are easily computed as these only involve propagators and worldline couplings.

The results for these diagrams are

$$\text{Diagram 4(a)} = 2Gq_1q_2m_2 \int dt \frac{3\vec{v}_2^2}{2r^2}, \quad (64)$$

$$\text{Diagram 4(b)} = Gq_1q_2m_2 \int dt \frac{\vec{v}_1 \cdot \vec{v}_2 - (\vec{n} \cdot \vec{v}_1)(\vec{n} \cdot \vec{v}_2)}{r}, \quad (65)$$

$$\text{Diagram 4(c)} = Gq_1q_2m_2 \int dt \frac{\vec{v}_1 \cdot \vec{v}_2 - (\vec{n} \cdot \vec{v}_1)(\vec{n} \cdot \vec{v}_2)}{r}, \quad (66)$$

$$\text{Diagram 4(d)} = 2Gq_1q_2m_2 \int dt_1 \frac{\vec{v}_1 \cdot \vec{v}_2}{r^2}, \quad (67)$$

$$\text{Diagram 4(e)} = -4Gq_1q_2m_2 \int dt_1 \frac{\vec{v}_1 \cdot \vec{v}_2}{r^2}, \quad (68)$$

$$\text{Diagram 4(f)} = -4Gq_1q_2m_2 \int dt_1 \frac{v_2^2}{r^2}. \quad (69)$$

The diagrams 4(g) and 4(h) involve a 3-point internal vertex and are calculated similarly to diagram 2(d). They are

$$\text{Diagram 4(g)} = Gq_1^2m_2 \int dt_1 \frac{-1}{4} \frac{(\vec{v}_1 \cdot \vec{v}_1 - 2(\vec{n} \cdot \vec{v}_1)(\vec{n} \cdot \vec{v}_1))}{r^2} - \frac{1}{4} \frac{v_1^2}{r^2}, \quad (70)$$

$$\text{Diagram 4(h)} = Gq_1m_1q_2 \int dt_1 \frac{(\vec{v}_1 \cdot \vec{v}_2 - \frac{1}{2}(\vec{n} \cdot \vec{v}_1)(\vec{n} \cdot \vec{v}_2))}{r^2}, \quad (71)$$

$$\text{Diagram 4(i)} = Gq_1^2m_2 \int dt_1 \frac{5}{8} \frac{(\vec{v}_1 \cdot \vec{v}_1 - 2(\vec{n} \cdot \vec{v}_1)(\vec{n} \cdot \vec{v}_1))}{r^2} - \frac{3}{8} \frac{\vec{v}_1 \cdot \vec{v}_2}{r^2} + 2 \frac{(\vec{v}_1 \cdot \vec{v}_2 - 2(\vec{n} \cdot \vec{v}_1)(\vec{n} \cdot \vec{v}_2))}{r^2}, \quad (72)$$

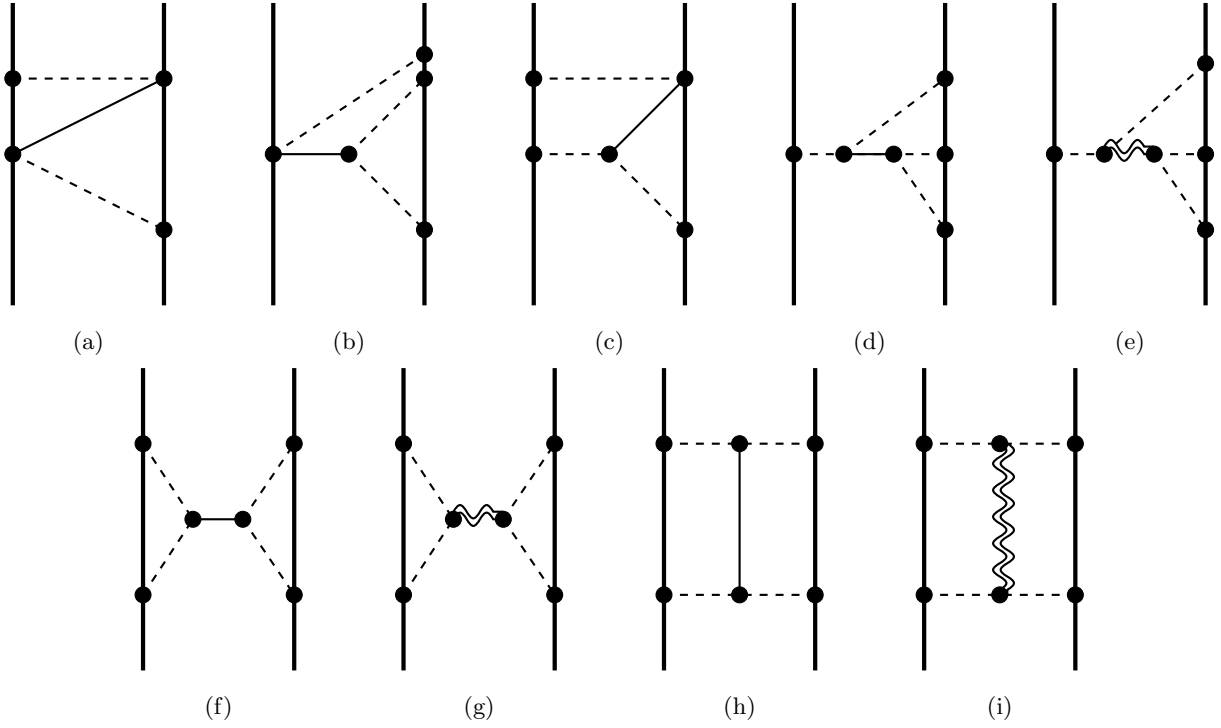
$$\text{Diagram 4(j)} = Gq_1^2m_2 \int dt_1 \frac{(\vec{v}_1 \cdot \vec{v}_2 - (\vec{n} \cdot \vec{v}_1)(\vec{n} \cdot \vec{v}_2))}{r^2}, \quad (73)$$

$$\text{Diagram 4(k)} = Gq_1q_2m_1 \int dt_1 \frac{(\vec{v}_1 \cdot \vec{v}_2 - 2(\vec{n} \cdot \vec{v}_1)(\vec{n} \cdot \vec{v}_2))}{r^2} - \frac{13}{8} \frac{(\vec{v}_1 \cdot \vec{v}_1 - 2(\vec{n} \cdot \vec{v}_1)(\vec{n} \cdot \vec{v}_1))}{r^2}, \quad (74)$$

$$\text{Diagram 4(l)} = Gq_1q_2m_1 \int dt_1 \frac{(\vec{v}_1 \cdot \vec{v}_2 - 2(\vec{n} \cdot \vec{v}_1)(\vec{n} \cdot \vec{v}_2))}{r^2}, \quad (75)$$

$$\text{Diagram 4(m)} = Gq_1q_2m_1 \int dt_1 \frac{11}{8} \frac{(\vec{v}_1 \cdot \vec{v}_2 - 2(\vec{n} \cdot \vec{v}_1)(\vec{n} \cdot \vec{v}_2))}{r^2} - \frac{1}{8} \frac{\vec{v}_1 \cdot \vec{v}_2}{r^2} - \frac{(\vec{v}_1 \cdot \vec{v}_1 - 2(\vec{n} \cdot \vec{v}_1)(\vec{n} \cdot \vec{v}_1))}{r^2}, \quad (76)$$

$$\text{Diagram 4(n)} = Gq_1q_2m_2 \int dt_1 \frac{3(\vec{v}_1 \cdot \vec{v}_2)}{r^2}, \quad (77)$$

FIG. 5: Diagrams that have $\mathcal{O}(Gq^4)$.

$$\text{Diagram 4(o)} = Gq_1q_2m_2 \int dt_1 \frac{3(\vec{v}_1 \cdot \vec{v}_2)}{r^2}, \quad (78)$$

$$\text{Diagram 4(p)} = -2Gq_1q_2m_2 \int dt_1 \frac{\vec{v}_2^2}{r^2}, \quad (79)$$

$$\text{Diagram 4(q)} = -4Gq_1q_2m_2 \int dt_1 \frac{v_2^2 + (\vec{v}_2 \cdot \vec{n})(\vec{v}_2 \cdot \vec{n})}{r^2}, \quad (80)$$

$$\text{Diagram 4(r)} = \frac{1}{2}Gq_2^2m_1 \int dt_1 \frac{5v_1^2 + (\vec{v}_1 \cdot \vec{n})(\vec{v}_1 \cdot \vec{n})}{r^2}, \quad (81)$$

$$\text{Diagram 4(s)} = -8Gq_1q_2m_2 \int dt_1 \frac{(\vec{v}_1 \cdot \vec{n})(\vec{v}_2 \cdot \vec{n})}{2r^2} - \frac{(\vec{v}_1 \cdot \vec{v}_2)}{r^2}, \quad (82)$$

$$\text{Diagram 4(t)} = -4Gq_1q_2m_2 \int dt_1 \frac{(\vec{v}_1 \cdot \vec{n})(\vec{v}_1 \cdot \vec{n})}{2r^2} - \frac{(\vec{v}_1 \cdot \vec{v}_1)}{r^2}. \quad (83)$$

C. Gq^4 order diagrams

The symmetry factors of diagrams 5(b), 5(d), 5(e), 5(h), and 5(i) in Fig. 5 are 1/2 and those of 5(f) and 5(g) are 1/4. The diagrams 5(d), 5(e) are nested 2-loop type, 5(f), 5(g) are factorizable 2-loop type and 5(h), 5(i) are irreducible 2-loop type.

The diagram 5(a) is easily computed using propagators and worldlines. The result is

$$\text{Diagram 5(a)} = 4Gq_1^2q_2^2 \int dt_1 \frac{1}{r^3}. \quad (84)$$

The diagrams 5(b) and 5(c) have a single 3-point vertex and are computed using the 1-loop master integral. Let us show this explicitly for diagram 5(b). We write the diagram in the usual manner using Eqs. (21), (19), and (42):

$$\text{Diagram 5(b)} = -2q_1 \int dt_1 A_0(x_1) \phi(x_1) (-q_2) \int dt_2 A_0(x_2) (-q_2) \int dt_3 A_0(x_2) (-q_2) \int dt_4 A_0(x_2) \frac{-1}{8\pi} \int d^4x 4\phi \partial^i A^0 \partial^j A^0 \delta_{ij}. \quad (85)$$

We appropriately contract the NRG fields and EM fields. Since there is no time derivative up to 2PN order, we use the relevant propagators and integrate over time all the delta functions in time. We integrate over d^3x which gives a delta function in momentum; integrating over these two momenta with delta function gives us

$$\text{Diagram 5(b)} = \alpha \int dt \frac{1}{4\pi r} \int_{k_2} \frac{e^{i\vec{k}_2 \cdot \vec{r}}}{\vec{k}_2^2} \int_{k_3} \frac{(k_2^i + k_3^i)k_3^j}{(\vec{k}_2 + \vec{k}_3)^2 \vec{k}_3^2} \delta_{ij}, \quad (86)$$

where $\alpha = 2q_1q_2^3(4\pi G)(-4\pi)^3/(-2\pi)$. We solve the integral over k_3 using the 1-loop master integrals A7,

$$\text{Diagram 5(b)} = \alpha \int dt \frac{1}{4\pi r} \int_{k_2} \frac{e^{i\vec{k}_2 \cdot \vec{r}}}{\vec{k}_2^2} \quad (87)$$

This integral is solved using identity A2 and gives following result,

$$\text{Diagram 5(b)} = Gq_1q_2^3 \int dt_1 \frac{1}{r^3}. \quad (88)$$

Diagram (c) can be computed similarly, leading to

$$\text{Diagram 5(c)} = 2Gq_1^2q_2^2 \int dt_1 \frac{1}{r^3}. \quad (89)$$

The diagrams (d) through (i) involve two 3-point vertices, which makes this type of diagram difficult to compute. As an illustration, let us explicitly compute the diagram (h). The diagram is constructed in the usual manner, using Eq. (19) and Eq. (42),

$$\begin{aligned} \text{Diagram 5(h)} &= \int dt_1 q_1 A_0(x_1) \int dt_2 q_1 A_0(x_1) \int dt_3 q_2 A_0(x_2) \int dt_4 q_2 A_0(x_2) \frac{-1}{8\pi} \int d^4x 4\phi \partial^i A^0 \partial^j A^0 \delta_{ij} \int dt_4 q_2 A_0(x_2) \\ &\times \frac{-1}{8\pi} \int d^4y 4\phi \partial^l A^0 \partial^m A^0 \delta_{lm}. \end{aligned} \quad (90)$$

We appropriately contract the NRG fields and EM fields. Also here, since there is no time derivative up to 2PN order, we use the relevant propagators and integrate over time all the delta functions in time. We then integrate over d^3x and d^3y , which gives delta functions in momenta. Integrating over these two momenta with delta functions gives us following expression:

$$\text{Diagram 5(h)} = \alpha \int dt \int_{k_1, k_2, k_3} e^{i(\vec{k}_1 + \vec{k}_3) \cdot \vec{r}} \frac{(\vec{k}_1 \cdot \vec{k}_2)(\vec{k}_3 \cdot (-\vec{k}_1 - \vec{k}_2 - \vec{k}_3))}{\vec{k}_1^2 \vec{k}_2^2 (\vec{k}_1 + \vec{k}_2)^2 \vec{k}_3^2 (\vec{k}_1 + \vec{k}_3)^2}, \quad (91)$$

where $\alpha = q_1^2q_2^2(4\pi G)(-4\pi)^4/(-2\pi)^2$. To further simplify the integral, we redefine the momenta as $\vec{k}_1 \rightarrow \vec{k}_1 + \vec{k}_3$ and $\vec{k}_2 \rightarrow \vec{k}_1 + \vec{k}_2$, which gives

$$\text{Diagram 5(h)} = \alpha \int dt \int_{k_1, k_2, k_3} e^{i\vec{k}_1 \cdot \vec{r}} \frac{(\vec{k}_1 - \vec{k}_3) \cdot (\vec{k}_2 - \vec{k}_1)(\vec{k}_3 \cdot \vec{k}_2)}{(\vec{k}_1 - \vec{k}_3)^2 \vec{k}_2^2 (\vec{k}_1 + \vec{k}_2)^2 \vec{k}_3^2 (\vec{k}_1 + \vec{k}_3)^2}. \quad (92)$$

This integral is irreducible. We further split the terms one by one and solve them individually:

$$\text{Diagram 5(h)} = \alpha \int dt \int_{k_1} e^{i\vec{k}_1 \cdot \vec{r}} (\mathbf{I}_1 + \mathbf{I}_2 + \mathbf{I}_3 + \mathbf{I}_4), \quad (93)$$

where the terms \mathbf{I}_1 , \mathbf{I}_2 , \mathbf{I}_3 , and \mathbf{I}_4 are defined as

$$\mathbf{I}_1 = \int_{k_2, k_3} \frac{(\vec{k}_1 \cdot \vec{k}_2)(\vec{k}_3 \cdot \vec{k}_2)}{(\vec{k}_1 - \vec{k}_3)^2 \vec{k}_2^2 (\vec{k}_1 + \vec{k}_2)^2 \vec{k}_3^2 (\vec{k}_1 + \vec{k}_3)^2}, \quad (94)$$

$$\mathbf{I}_2 = \int_{k_2, k_3} \frac{(-\vec{k}_1 \cdot \vec{k}_1)(\vec{k}_3 \cdot \vec{k}_2)}{(\vec{k}_1 - \vec{k}_3)^2 \vec{k}_2^2 (\vec{k}_1 + \vec{k}_2)^2 \vec{k}_3^2 (\vec{k}_1 + \vec{k}_3)^2}, \quad (95)$$

$$\mathbf{I}_3 = \int_{k_2, k_3} \frac{(-\vec{k}_3 \cdot \vec{k}_2)(\vec{k}_3 \cdot \vec{k}_2)}{(\vec{k}_1 - \vec{k}_3)^2 \vec{k}_2^2 (\vec{k}_1 + \vec{k}_2)^2 \vec{k}_3^2 (\vec{k}_1 + \vec{k}_3)^2}, \quad (96)$$

$$\mathbf{I}_4 = \int_{k_2, k_3} \frac{(\vec{k}_3 \cdot \vec{k}_1)(\vec{k}_3 \cdot \vec{k}_2)}{(\vec{k}_1 - \vec{k}_3)^2 \vec{k}_2^2 (\vec{k}_1 + \vec{k}_2)^2 \vec{k}_3^2 (\vec{k}_1 + \vec{k}_3)^2}. \quad (97)$$

We encounter infinity while doing this integral, which can be taken care of by using regularization. We compute the integral in $3 - \epsilon$ dimensions and in the final result take the limit $\epsilon \rightarrow 0$, which gives a finite result. We solve the sub-integrals using Eq. (A12), which gives the final result:

$$\text{Diagram 5(h)} = -\frac{(16 \times 17)}{4} G q_1^2 q_2^2 \int dt_1 \frac{1}{r^3}. \quad (98)$$

Similarly,

$$\text{Diagram 5(d)} = -\frac{1}{3} G q_1 q_2^3 \int dt_1 \frac{1}{r^3}, \quad (99)$$

$$\text{Diagram 5(e)} = \frac{1002}{6} G q_1 q_2^3 \int dt_1 \frac{1}{r^3}, \quad (100)$$

The factorizable 2-loop diagrams 5(f) and 5(g) yield short distance contributions which cancel out:

$$\text{Diagram 5(f)} = 0, \quad (101)$$

$$\text{Diagram 5(g)} = 0, \quad (102)$$

$$\text{Diagram 5(i)} = \frac{258}{2} G q_1 q_2^3 \int dt_1 \frac{1}{r^3}. \quad (103)$$

D. $G^2 q^2$ order diagrams

The symmetry factors of diagrams 6(e), 6(h), 6(i), 6(j), 6(o), 6(p) are 1/2, the one for diagram 6(l) is 1/4, and the rest of the diagrams have symmetry factor 1. The diagrams 6(i), 6(j), 6(m), 6(n) are nested 2-loop type, 6(k), 6(l), 6(o) are factorizable 2-loop type and 6(p), 6(q) are irreducible 2-loop type.

The diagrams 6(a) and 6(b) are easily computed using propagators and worldlines. The results are:

$$\text{Diagram 6(a)} = -2G^2 q_1 q_2 m_2^2 \int dt_1 \frac{1}{r^3}, \quad (104)$$

$$\text{Diagram 6(b)} = G^2 q_1 q_2 m_1 m_2 \int dt_1 \frac{1}{r^3}, \quad (105)$$

$$\text{Diagram 6(c)} = -4G^2 q_1 q_2 m_1 m_2 \int dt_1 \frac{1}{r^3}. \quad (106)$$

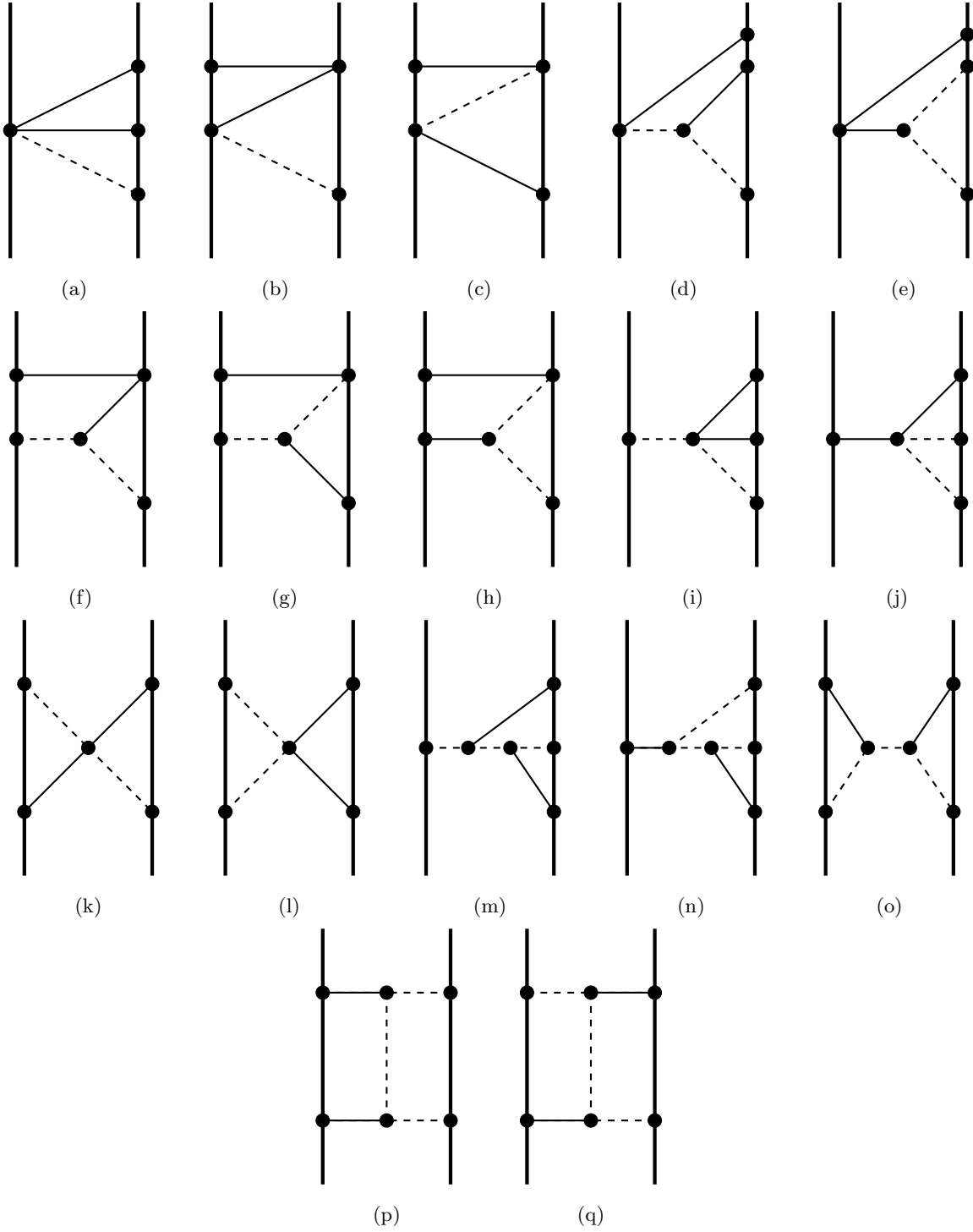


FIG. 6: Diagrams that have $\mathcal{O}(G^2 q^2)$.

The diagrams (c), (d), (e) and (f) have one 3-point vertex, which is solved using the 1-loop master integral (A7) similarly to diagram 5(b). The results are:

$$\text{Diagram 6(d)} = -2G^2 q_1 q_2 m_2^2 \int dt_1 \frac{1}{r^3}, \quad (107)$$

$$\text{Diagram 6(e)} = G^2 q_2^2 m_1 m_2 \int dt_1 \frac{1}{4r^3}, \quad (108)$$

$$\text{Diagram 6(f)} = -G^2 q_1 q_2 m_1 m_2 \int dt_1 \frac{1}{2r^3}, \quad (109)$$

$$\text{Diagram 6(g)} = -2G^2 q_1 q_2 m_1 m_2 \int dt_1 \frac{1}{r^3}, \quad (110)$$

$$\text{Diagram 6(h)} = G^2 q_2^2 m_1^2 \int dt_1 \frac{1}{r^3}, \quad (111)$$

The diagrams (i), (j), (k) and (l) involve a single 4-point vertex. We show how to compute one of the diagrams, namely (g). The diagram is constructed in the usual manner, using Eq. (19), Eq. (11) and Eq. (47):

$$\text{Diagram 6(i)} = \int dt_1 (-q_1) A_0(x_1) \int dt_2 (-q_1) A_0(x_2) \int dt_3 (-m_2) \phi(x_2) \int dt_4 (-m_2) \phi(x_2) \frac{-1}{4\pi} \int d^4x (-4)(\partial^i A^0)^2 \phi^2. \quad (112)$$

As before,

$$\text{Diagram 6(i)} = G^2 q_1 q_2 m_2^2 \frac{1}{\pi} (-4\pi)^2 \int dt_1 \frac{1}{r^2} \int_{k_1} \frac{e^{i\vec{k}_1 \cdot \vec{r}}}{\vec{k}_1^2}. \quad (113)$$

After carrying out the Fourier integral using Eq. (A2), we get final result:

$$\text{Diagram 6(i)} = 2G^2 q_1 q_2 m_2^2 \int dt_1 \frac{1}{r^3}. \quad (114)$$

The remaining three diagrams, (j), (k), and (l), are evaluated similarly. The results are

$$\text{Diagram 6(j)} = 2G^2 q_2^2 m_1 m_2 \int dt_1 \frac{1}{r^3}, \quad (115)$$

The factorizable 2-loop diagrams 6(k), 6(l) and 6(o) yield short distance contributions which cancel out:

$$\text{Diagram 6(k)} = 0, \quad (116)$$

$$\text{Diagram 6(l)} = 0. \quad (117)$$

The diagrams (m), (n), (o), (p), and (q) involve two 3-point vertices. These diagrams are calculated similarly to diagram 5(j), resulting in

$$\text{Diagram 6(m)} = -\frac{4}{3} G^2 q_1 q_2 m_2^2 \int dt_1 \frac{1}{r^3}, \quad (118)$$

$$\text{Diagram 6(n)} = -2G^2 m_1 m_2 q_2^2 \int dt_1 \frac{1}{r^3}, \quad (119)$$

$$\text{Diagram 6(o)} = 0, \quad (120)$$

$$\text{Diagram 6(p)} = -G^2 q_2^2 m_1 m_2 \int dt_1 \frac{1}{4r^3}, \quad (121)$$

$$\text{Diagram 6(q)} = -G^2 q_2^2 m_1 m_2 \int dt_1 \frac{1}{2r^3}. \quad (122)$$

VI. RESULTS

Having computed all the diagrams, we can now construct the 2PN interaction Lagrangian. There are two contributions which we need. The first is the kinetic energy, which is obtained by expanding the matter coupling action, Eq. (10), to $\mathcal{O}(v^6)$ while setting all fields to zero. The final potential is obtained by summing each potential contribution from the diagrams.

The Lagrangian at 1PN order including kinetic energy term is given by

$$\mathcal{L}_{1PN} = \frac{1}{8}m_1v_1^4 + \frac{-q_1q_2}{r}\frac{q_1q_2}{r}(\vec{v}_1 \cdot \vec{v}_2) - \frac{q_1q_2}{2r}\left(\vec{v}_1 \cdot \vec{v}_2 - \frac{(\vec{v}_1 \cdot \vec{r})(\vec{v}_2 \cdot \vec{r})}{r^2}\right) + \frac{Gq_1q_2}{r^2}(m_2 + m_1) - \frac{G}{2r^2}(m_2q_1^2 + m_1q_2^2). \quad (123)$$

For the Lagrangian at 2PN order we need to add the further contributions found above; it is given by

$$\begin{aligned} \mathcal{L}_{2PN} = & \frac{1}{16}m_1v_1^6 + \frac{q_1q_2}{2r}\left(\vec{v}_1 \cdot \vec{v}_2 - \frac{(\vec{v}_1 \cdot \vec{r})(\vec{v}_2 \cdot \vec{r})}{r^2}\right)(\vec{v}_1 \cdot \vec{v}_2) + 2q_1q_2\left(\frac{3(\vec{n} \cdot \vec{v}_1)^2(\vec{n} \cdot \vec{v}_2)^2}{16r} + \frac{2(\vec{v}_1 \cdot \vec{v}_2)^2 + \vec{v}_1^2\vec{v}_2^2}{16r}\right. \\ & \left. - \frac{4(\vec{n} \cdot \vec{v}_1)(\vec{n} \cdot \vec{v}_2)(\vec{v}_1 \cdot \vec{v}_2)}{16r} - \frac{(\vec{n} \cdot \vec{v}_1)^2\vec{v}_2^2 - (\vec{n} \cdot \vec{v}_2)^2\vec{v}_1^2}{16r}\right) + 2Gq_1q_2m_2\frac{3\vec{v}_2^2}{2r^2} + Gq_1q_2m_2\frac{\vec{v}_1 \cdot \vec{v}_2 - (\vec{n} \cdot \vec{v}_1)(\vec{n} \cdot \vec{v}_2)}{r} \\ & Gq_1q_2m_2\frac{\vec{v}_1 \cdot \vec{v}_2 - (\vec{n} \cdot \vec{v}_1)(\vec{n} \cdot \vec{v}_2)}{r} + 2Gq_1q_2m_2\frac{\vec{v}_1 \cdot \vec{v}_2}{r^2} - 4Gq_1q_2m_2\frac{\vec{v}_1 \cdot \vec{v}_2}{r^2} - 4Gq_1q_2m_2\frac{v_2^2}{r^2} \\ & + Gq_1^2m_2\left(\frac{-1}{4}\frac{(\vec{v}_1 \cdot \vec{v}_1 - 2(\vec{n} \cdot \vec{v}_1)(\vec{n} \cdot \vec{v}_1))}{r^2} - \frac{1}{4}\frac{v_1^2}{r^2}\right) + Gq_1m_1q_2\frac{(\vec{v}_1 \cdot \vec{v}_2 - \frac{1}{2}(\vec{n} \cdot \vec{v}_1)(\vec{n} \cdot \vec{v}_2))}{r^2} \\ & + Gq_1^2m_2\left(\frac{5}{8}\frac{(\vec{v}_1 \cdot \vec{v}_1 - 2(\vec{n} \cdot \vec{v}_1)(\vec{n} \cdot \vec{v}_1))}{r^2} - \frac{3}{8}\frac{\vec{v}_1 \cdot \vec{v}_2}{r^2} + 2\frac{(\vec{v}_1 \cdot \vec{v}_2 - 2(\vec{n} \cdot \vec{v}_1)(\vec{n} \cdot \vec{v}_2))}{r^2}\right) + Gq_1^2m_2\frac{(\vec{v}_1 \cdot \vec{v}_2 - (\vec{n} \cdot \vec{v}_1)(\vec{n} \cdot \vec{v}_2))}{r^2} \\ & + Gq_1q_2m_1\left(\frac{(\vec{v}_1 \cdot \vec{v}_2 - 2(\vec{n} \cdot \vec{v}_1)(\vec{n} \cdot \vec{v}_2))}{r^2} - \frac{13}{8}\frac{(\vec{v}_1 \cdot \vec{v}_1 - 2(\vec{n} \cdot \vec{v}_1)(\vec{n} \cdot \vec{v}_1))}{r^2}\right) + Gq_1q_2m_1\frac{(\vec{v}_1 \cdot \vec{v}_2 - 2(\vec{n} \cdot \vec{v}_1)(\vec{n} \cdot \vec{v}_2))}{r^2} \\ & + Gq_1q_2m_1\left(\frac{11}{8}\frac{(\vec{v}_1 \cdot \vec{v}_2 - 2(\vec{n} \cdot \vec{v}_1)(\vec{n} \cdot \vec{v}_2))}{r^2} - \frac{1}{8}\frac{\vec{v}_1 \cdot \vec{v}_2}{r^2} - \frac{(\vec{v}_1 \cdot \vec{v}_1 - 2(\vec{n} \cdot \vec{v}_1)(\vec{n} \cdot \vec{v}_1))}{r^2}\right) + Gq_1q_2m_2\frac{3(\vec{v}_1 \cdot \vec{v}_2)}{r^2} \\ & + Gq_1q_2m_2\frac{3(\vec{v}_1 \cdot \vec{v}_2)}{r^2} - 2Gq_1q_2m_2\frac{\vec{v}_2^2}{r^2} - 4Gq_1q_2m_2\frac{v_2^2 + (\vec{v}_2 \cdot \vec{n})(\vec{v}_2 \cdot \vec{n})}{r^2} + \frac{1}{2}Gq_2^2m_1\frac{5v_1^2 + (\vec{v}_1 \cdot \vec{n})(\vec{v}_1 \cdot \vec{n})}{r^2} \\ & - 8Gq_1q_2m_2\left(\frac{(\vec{v}_1 \cdot \vec{n})(\vec{v}_2 \cdot \vec{n})}{2r^2} - \frac{(\vec{v}_1 \cdot \vec{v}_2)}{r^2}\right) - 4Gq_1q_2m_2\left(\frac{(\vec{v}_1 \cdot \vec{n})(\vec{v}_1 \cdot \vec{n})}{2r^2} - \frac{(\vec{v}_1 \cdot \vec{v}_1)}{r^2}\right) + 4Gq_1^2q_2^2\frac{1}{r^3} + Gq_1q_2^3\frac{1}{r^3} + 2Gq_1^2q_2^2\frac{1}{r^3} \\ & - \frac{1}{3}Gq_1q_2^3\frac{1}{r^3} + \frac{1002}{6}Gq_1q_2^3\frac{1}{r^3} + \frac{258}{2}Gq_1q_2^3\frac{1}{r^3} - \frac{(16 \times 17)}{4}Gq_1^2q_2^2\frac{1}{r^3} - 2G^2q_1q_2m_2^2\frac{1}{r^3} + G^2q_1q_2m_1m_2\frac{1}{r^3} - 4G^2q_1q_2m_1m_2\frac{1}{r^3} \\ & - 2G^2q_1q_2m_2^2\frac{1}{r^3} + G^2q_2^2m_1m_2\frac{1}{4r^3} - G^2q_1q_2m_1m_2\frac{1}{2r^3} - 2G^2q_1q_2m_1m_2\frac{1}{r^3} + G^2q_2^2m_1^2\frac{1}{r^3} + 2G^2q_1q_2m_2^2\frac{1}{r^3} \\ & + 2G^2q_2^2m_1m_2\frac{1}{r^3} - \frac{4}{3}G^2q_1q_2m_2^2\frac{1}{r^3} - 2G^2m_1m_2q_2^2\frac{1}{r^3} - G^2q_2^2m_1m_2\frac{1}{4r^3} - G^2q_2^2m_1m_2\frac{1}{2r^3}, \quad (124) \end{aligned}$$

where one has to add the contribution from changing $1 \leftrightarrow 2$ and $\vec{n} \rightarrow -\vec{n}$.

VII. CONCLUSIONS

We have described how to use the EFT method to efficiently calculate the 2PN order Lagrangian of Einstein-Maxwell theory for a binary system. We have shown how to derive the Feynman rules up to 2PN order and have drawn the 1PN and 2PN order Feynman diagrams that contribute to the calculation of the Lagrangian. The calculation involved $\mathcal{O}(q^2v^4)$, $\mathcal{O}(Gq^2v^2)$, $\mathcal{O}(G^2q^2)$ and $\mathcal{O}(Gq^4)$ kinds of 2PN order diagrams. These include 1-loop and 2-loop integrals. All diagrams could be computed with only two master integrals. This demonstrates the efficiency of the EFT method for the calculation of the 2PN Lagrangian.

An obvious extension of the current result is to compute the 3PN Lagrangian, which will involve upto 3-loop Feynman integrals; the number of diagrams to be evaluated is large, and we leave this for future work. Finally, with a Lagrangian in hand, a next step will be to calculate the orbital motion, and the gravitational radiation that will be emitted; this is work in progress.

ACKNOWLEDGMENTS

The author is very grateful to Jan Steinhoff for suggesting EFT method and valuable discussions throughout the project. The author would also like to thank Chris Van Den Broeck for going through the manuscript. The author thanks Tanja Hinderer and Jasper Roosmale Nepveu for valuable comments to improve the manuscript. This work was supported by the Netherlands Organization for Scientific Research (NWO).

Appendix A: Useful formulas

We flip the time derivative between the two particles by using the identity

$$\int dt_1 dt_2 \partial_{t_1} \delta(t_1 - t_2) f(t_1) g(t_2) = - \int dt_1 dt_2 \partial_{t_2} \delta(t_1 - t_2) f(t_1) g(t_2). \quad (\text{A1})$$

We evaluate the Fourier integrals which we often encounter from propagators and loop integrals using the d-dimensional master formula given by

$$\int \frac{d^d \mathbf{k}}{(2\pi)^d} \frac{e^{i\mathbf{k}\cdot\mathbf{r}}}{(\mathbf{k}^2)^\alpha} = \frac{1}{(4\pi)^{d/2}} \frac{\Gamma(d/2 - \alpha)}{\Gamma(\alpha)} \left(\frac{\mathbf{r}^2}{4}\right)^{\alpha-d/2}. \quad (\text{A2})$$

From this master formula, we obtain the following required Fourier integrals [38]:

$$I^i \equiv \int \frac{d^d \mathbf{k}}{(2\pi)^d} \frac{k^i e^{i\mathbf{k}\cdot\mathbf{r}}}{(\mathbf{k}^2)^\alpha} = \frac{i}{(4\pi)^{d/2}} \frac{\Gamma(d/2 - \alpha + 1)}{\Gamma(\alpha)} \left(\frac{\mathbf{r}^2}{4}\right)^{\alpha-d/2-1/2} n^i, \quad (\text{A3})$$

$$I^{ij} \equiv \int \frac{d^d \mathbf{k}}{(2\pi)^d} \frac{k^i k^j e^{i\mathbf{k}\cdot\mathbf{r}}}{(\mathbf{k}^2)^\alpha} = \frac{1}{(4\pi)^{d/2}} \frac{\Gamma(d/2 - \alpha + 1)}{\Gamma(\alpha)} \left(\frac{\mathbf{r}^2}{4}\right)^{\alpha-d/2-1} \left(\frac{1}{2} \delta^{ij} + (\alpha - 1 - d/2) n^i n^j\right), \quad (\text{A4})$$

$$I^{ijl} \equiv \int \frac{d^d \mathbf{k}}{(2\pi)^d} \frac{k^i k^j k^l e^{i\mathbf{k}\cdot\mathbf{r}}}{(\mathbf{k}^2)^\alpha} = \frac{i}{(4\pi)^{d/2}} \frac{\Gamma(d/2 - \alpha + 2)}{\Gamma(\alpha)} \left(\frac{\mathbf{r}^2}{4}\right)^{\alpha-d/2-3/2} \times \left(\frac{1}{2} (\delta^{ij} n^l + \delta^{il} n^j + \delta^{jl} n^i) + (\alpha - d/2 - 2) n^i n^j n^l\right), \quad (\text{A5})$$

$$I^{ijlm} \equiv \int \frac{d^d \mathbf{k}}{(2\pi)^d} \frac{k^i k^j k^l k^m e^{i\mathbf{k}\cdot\mathbf{r}}}{(\mathbf{k}^2)^\alpha} = \frac{1}{(4\pi)^{d/2}} \frac{\Gamma(d/2 - \alpha + 2)}{\Gamma(\alpha)} \left(\frac{\mathbf{r}^2}{4}\right)^{\alpha-d/2-2} \left(\frac{1}{4} (\delta^{ij} \delta^{lm} + \delta^{il} \delta^{jm} + \delta^{im} \delta^{jl}) \right. \\ \left. + \frac{\alpha - d/2 - 2}{2} (\delta^{ij} n^l n^m + \delta^{il} n^j n^m + \delta^{im} n^j n^l + \delta^{jl} n^i n^m + \delta^{jm} n^i n^l + \delta^{lm} n^i n^j) \right. \\ \left. + (\alpha - d/2 - 2)(\alpha - d/2 - 3) n^i n^j n^l n^m\right). \quad (\text{A6})$$

We use the d-dimensional master formula for one-loop scalar integrals given by

$$J \equiv \int \frac{d^d \mathbf{k}}{(2\pi)^d} \frac{1}{[\mathbf{k}^2]^\alpha [(\mathbf{k} - \mathbf{q})^2]^\beta} = \frac{1}{(4\pi)^{d/2}} \frac{\Gamma(\alpha + \beta - d/2)}{\Gamma(\alpha)\Gamma(\beta)} \frac{\Gamma(d/2 - \alpha)\Gamma(d/2 - \beta)}{\Gamma(d - \alpha - \beta)} (q^2)^{d/2 - \alpha - \beta}. \quad (\text{A7})$$

The d-dimensional master formula for one-loop tensor integrals is also taken from [38]. Similarly, one can also derive the following d-dimensional master formulae for the one-loop tensor integrals:

$$J^i \equiv \int \frac{d^d \mathbf{k}}{(2\pi)^d} \frac{k^i}{[\mathbf{k}^2]^\alpha [(\mathbf{k} - \mathbf{q})^2]^\beta} = \frac{1}{(4\pi)^{d/2}} \frac{\Gamma(\alpha + \beta - d/2)}{\Gamma(\alpha)\Gamma(\beta)} \frac{\Gamma(d/2 - \alpha + 1)\Gamma(d/2 - \beta)}{\Gamma(d - \alpha - \beta + 1)} (q^2)^{d/2 - \alpha - \beta} q^i, \quad (\text{A8})$$

$$J^{ij} \equiv \int \frac{d^d \mathbf{k}}{(2\pi)^d} \frac{k^i k^j}{[\mathbf{k}^2]^\alpha [(\mathbf{k} - \mathbf{q})^2]^\beta} = \frac{1}{(4\pi)^{d/2}} \frac{\Gamma(\alpha + \beta - d/2 - 1)}{\Gamma(\alpha)\Gamma(\beta)} \frac{\Gamma(d/2 - \alpha + 1)\Gamma(d/2 - \beta)}{\Gamma(d - \alpha - \beta + 2)} (q^2)^{d/2 - \alpha - \beta} \\ \times \left(\frac{d/2 - \beta}{2} q^2 \delta^{ij} + (\alpha + \beta - d/2 - 1)(d/2 - \alpha + 1) q^i q^j\right), \quad (\text{A9})$$

$$J^{ijl} \equiv \int \frac{d^d \mathbf{k}}{(2\pi)^d} \frac{k^i k^j k^l}{[\mathbf{k}^2]^\alpha [(\mathbf{k} - \mathbf{q})^2]^\beta} = \frac{1}{(4\pi)^{d/2}} \frac{\Gamma(\alpha + \beta - d/2 - 1)}{\Gamma(\alpha)\Gamma(\beta)} \frac{\Gamma(d/2 - \alpha + 2)\Gamma(d/2 - \beta)}{\Gamma(d - \alpha - \beta + 3)} (q^2)^{d/2 - \alpha - \beta} \\ \times \left(\frac{d/2 - \beta}{2} q^2 (\delta^{ij} q^l + \delta^{il} q^j + \delta^{jl} q^i) \right. \\ \left. + (\alpha + \beta - d/2 - 1)(d/2 - \alpha + 2) q^i q^j q^l\right), \quad (\text{A10})$$

$$\begin{aligned}
J^{ijlm} \equiv \int \frac{d^d \mathbf{k}}{(2\pi)^d} \frac{k^i k^j k^l k^m}{[\mathbf{k}^2]^\alpha [(\mathbf{k} - \mathbf{q})^2]^\beta} = & \frac{1}{(4\pi)^{d/2}} \frac{\Gamma(\alpha + \beta - d/2 - 2) \Gamma(d/2 - \alpha + 2) \Gamma(d/2 - \beta)}{\Gamma(\alpha) \Gamma(\beta)} (q^2)^{d/2 - \alpha - \beta} \\
& \times \left(\frac{(d/2 - \beta)(d/2 - \beta + 1)}{4} q^4 (\delta^{ij} \delta^{lm} + \delta^{il} \delta^{jm} + \delta^{jl} \delta^{im}) \right. \\
& + (\alpha + \beta - d/2 - 2)(d/2 - \alpha + 2) \frac{d/2 - \beta}{2} q^2 \\
& \times (\delta^{ij} q^l q^m + \delta^{il} q^j q^m + \delta^{im} q^j q^l + \delta^{jl} q^i q^m + \delta^{jm} q^i q^l + \delta^{lm} q^i q^j) \\
& \left. + (\alpha + \beta - d/2 - 2)(\alpha + \beta - d/2 - 1)(d/2 - \alpha + 2)(d/2 - \alpha + 3) \right. \\
& \left. \times q^i q^j q^l q^m \right). \quad (\text{A11})
\end{aligned}$$

In addition, we encounter irreducible two-loop tensor integrals up to order 4. Using an integration by parts method as in [48], these can be written as a sum of factorizable and nested two-loops, as explained in Sec. [VC,VD](#). The required irreducible two-loop tensor integral reductions are given by

$$\begin{aligned}
\int_{\mathbf{k}_1 \mathbf{k}_2} \frac{k_1^i k_2^j}{k_1^2 (p - k_1)^2 k_2^2 (p - k_2)^2 (k_1 - k_2)^2} = & \frac{1}{d - 3} \int_{\mathbf{k}_1 \mathbf{k}_2} \left[\frac{p^i k_2^j}{k_1^4 (p - k_1)^2 k_2^2 (p - k_2)^2} - \frac{k_1^i k_2^j}{k_1^4 (p - k_1)^2 (p - k_2)^2 (k_1 - k_2)^2} \right. \\
& - \frac{k_1^i k_2^j}{k_1^2 (p - k_1)^4 k_2^2 (k_1 - k_2)^2} + \frac{1}{d - 4} \left(2 \frac{k_2^i k_2^j}{k_1^4 (p - k_1)^2 k_2^2 (p - k_2)^2} \right. \\
& \left. \left. - \frac{k_2^i k_2^j}{k_1^4 (p - k_1)^2 (p - k_2)^2 (k_1 - k_2)^2} - \frac{k_2^i k_2^j}{k_1^2 (p - k_1)^4 k_2^2 (k_1 - k_2)^2} \right) \right], \quad (\text{A12})
\end{aligned}$$

$$\begin{aligned}
\int_{\mathbf{k}_1 \mathbf{k}_2} \frac{k_1^i k_1^j k_2^l}{k_1^2 (p - k_1)^2 k_2^2 (p - k_2)^2 (k_1 - k_2)^2} = & \frac{1}{d - 3} \int_{\mathbf{k}_1 \mathbf{k}_2} \left[\frac{p^l k_1^i k_1^j}{k_1^2 (p - k_1)^2 k_2^4 (p - k_2)^2} - \frac{k_1^i k_1^j k_2^l}{(p - k_1)^2 k_2^4 (p - k_2)^2 (k_1 - k_2)^2} \right. \\
& - \frac{k_1^i k_1^j k_2^l}{k_1^2 k_2^2 (p - k_2)^4 (k_1 - k_2)^2} + \frac{1}{d - 4} \left(2 \frac{k_1^i k_1^j k_1^l}{k_1^2 (p - k_1)^2 k_2^4 (p - k_2)^2} \right. \\
& \left. \left. - \frac{k_1^i k_1^j k_1^l}{(p - k_1)^2 k_2^4 (p - k_2)^2 (k_1 - k_2)^2} - \frac{k_1^i k_1^j k_1^l}{k_1^2 k_2^2 (p - k_2)^4 (k_1 - k_2)^2} \right) \right], \quad (\text{A13})
\end{aligned}$$

$$\begin{aligned}
\int_{\mathbf{k}_1 \mathbf{k}_2} \frac{k_1^i k_1^j k_2^l k_2^m}{k_1^2 (p - k_1)^2 k_2^2 (p - k_2)^2 (k_1 - k_2)^2} = & \frac{1}{d - 2} \int_{\mathbf{k}_1 \mathbf{k}_2} \left[\frac{k_1^i k_1^j k_2^l k_2^m}{k_1^4 (p - k_1)^2 k_2^2 (p - k_2)^2} + \frac{k_1^i k_1^j k_2^l k_2^m}{k_1^2 (p - k_1)^4 k_2^2 (p - k_2)^2} \right. \\
& - \frac{k_1^i k_1^j k_2^l k_2^m}{k_1^4 (p - k_1)^2 (p - k_2)^2 (k_1 - k_2)^2} - \frac{k_1^i k_1^j k_2^l k_2^m}{k_1^2 (p - k_1)^4 k_2^2 (k_1 - k_2)^2} \\
& + \frac{1}{d - 3} \left(\frac{p^i k_2^j k_2^l k_2^m}{k_1^4 (p - k_1)^2 k_2^2 (p - k_2)^2} + \frac{p^j k_2^i k_2^l k_2^m}{k_1^4 (p - k_1)^2 k_2^2 (p - k_2)^2} \right. \\
& - \frac{k_1^i k_2^j k_2^l k_2^m}{k_1^4 (p - k_1)^2 (p - k_2)^2 (k_1 - k_2)^2} - \frac{k_1^j k_2^i k_2^l k_2^m}{k_1^4 (p - k_1)^2 (p - k_2)^2 (k_1 - k_2)^2} \\
& - \frac{k_1^i k_2^j k_2^l k_2^m}{k_1^2 (p - k_1)^4 k_2^2 (k_1 - k_2)^2} - \frac{k_1^j k_2^i k_2^l k_2^m}{k_1^2 (p - k_1)^4 k_2^2 (k_1 - k_2)^2} \\
& \left. \left. + \frac{2}{d - 4} \left(2 \frac{k_2^i k_2^j k_2^l k_2^m}{k_1^4 (p - k_1)^2 k_2^2 (p - k_2)^2} - \frac{k_2^i k_2^j k_2^l k_2^m}{k_1^4 (p - k_1)^2 (p - k_2)^2 (k_1 - k_2)^2} \right. \right. \right. \\
& \left. \left. \left. - \frac{k_2^i k_2^j k_2^l k_2^m}{k_1^2 (p - k_1)^4 k_2^2 (k_1 - k_2)^2} \right) \right) \right]. \quad (\text{A14})
\end{aligned}$$

It should be noted that these expressions contain explicit poles in $d = 3$, but these cancel out in the dimensional regularization.

-
- [1] J. Aasi *et al.* (LIGO Scientific), *Class. Quant. Grav.* **32**, 074001 (2015), arXiv:1411.4547 [gr-qc].
 - [2] F. Acernese *et al.* (VIRGO), *Class. Quant. Grav.* **32**, 024001 (2015), arXiv:1408.3978 [gr-qc].
 - [3] B. P. Abbott *et al.* (LIGO Scientific, Virgo), *Phys. Rev. X* **6**, 041015 (2016), [Erratum: *Phys.Rev.X* 8, 039903 (2018)], arXiv:1606.04856 [gr-qc].
 - [4] B. P. Abbott *et al.* (LIGO Scientific, Virgo), *Phys. Rev. Lett.* **116**, 061102 (2016), arXiv:1602.03837 [gr-qc].
 - [5] B. P. Abbott *et al.* (LIGO Scientific, Virgo), *Phys. Rev. X* **9**, 031040 (2019), arXiv:1811.12907 [astro-ph.HE].
 - [6] R. Abbott *et al.* (LIGO Scientific, Virgo), *Phys. Rev. X* **11**, 021053 (2021), arXiv:2010.14527 [gr-qc].
 - [7] R. Abbott *et al.* (LIGO Scientific, VIRGO, KAGRA), (2021), arXiv:2111.03606 [gr-qc].
 - [8] P. K. Gupta, T. F. M. Spieksma, P. T. H. Pang, G. Koekoek, and C. V. D. Broeck, *Phys. Rev. D* **104**, 063041 (2021), arXiv:2107.12111 [gr-qc].
 - [9] P. Pani, E. Berti, and L. Gualtieri, *Phys. Rev. Lett.* **110**, 241103 (2013), arXiv:1304.1160 [gr-qc].
 - [10] P. Pani, E. Berti, and L. Gualtieri, *Phys. Rev. D* **88**, 064048 (2013), arXiv:1307.7315 [gr-qc].
 - [11] M. Zilhão, V. Cardoso, C. Herdeiro, L. Lehner, and U. Sperhake, *Phys. Rev. D* **90**, 124088 (2014), arXiv:1410.0694 [gr-qc].
 - [12] Z. Mark, H. Yang, A. Zimmerman, and Y. Chen, *Phys. Rev. D* **91**, 044025 (2015), arXiv:1409.5800 [gr-qc].
 - [13] O. J. C. Dias, M. Godazgar, and J. E. Santos, *Phys. Rev. Lett.* **114**, 151101 (2015), arXiv:1501.04625 [gr-qc].
 - [14] O. J. C. Dias, M. Godazgar, J. E. Santos, G. Carullo, W. Del Pozzo, and D. Laghi, (2021), arXiv:2109.13949 [gr-qc].
 - [15] G. Carullo, D. Laghi, N. K. Johnson-McDaniel, W. Del Pozzo, O. J. C. Dias, M. Godazgar, and J. E. Santos, (2021), arXiv:2109.13961 [gr-qc].
 - [16] L. Blanchet, *Fundam. Theor. Phys.* **162**, 125 (2011), arXiv:0907.3596 [gr-qc].
 - [17] L. Blanchet, *Living Rev. Rel.* **17**, 2 (2014), arXiv:1310.1528 [gr-qc].
 - [18] R. Patil, *Gen. Rel. Grav.* **52**, 95 (2020), arXiv:2009.11107 [gr-qc].
 - [19] M. Khalil, N. Sennett, J. Steinhoff, J. Vines, and A. Buonanno, *Phys. Rev. D* **98**, 104010 (2018), arXiv:1809.03109 [gr-qc].
 - [20] M. Punturo *et al.*, *Class. Quant. Grav.* **27**, 084007 (2010).
 - [21] S. Hild *et al.*, *Class. Quant. Grav.* **28**, 094013 (2011), arXiv:1012.0908 [gr-qc].
 - [22] B. P. Abbott *et al.* (LIGO Scientific), *Class. Quant. Grav.* **34**, 044001 (2017), arXiv:1607.08697 [astro-ph.IM].
 - [23] P. Amaro-Seoane *et al.*, arXiv e-prints, arXiv:1702.00786 (2017), arXiv:1702.00786 [astro-ph.IM].
 - [24] J. Baker *et al.*, (2019), arXiv:1907.06482 [astro-ph.IM].
 - [25] P. Amaro-Seoane *et al.*, (2022), arXiv:2203.06016 [gr-qc].
 - [26] W. D. Goldberger and I. Z. Rothstein, *Phys. Rev. D* **73**, 104029 (2006), arXiv:hep-th/0409156.
 - [27] W. D. Goldberger, in *Les Houches Summer School - Session 86: Particle Physics and Cosmology: The Fabric of Spacetime* (2007) arXiv:hep-ph/0701129.
 - [28] J. Blümlein, A. Maier, P. Marquard, and G. Schäfer, (2021), arXiv:2110.13822 [gr-qc].
 - [29] J.-W. Kim, M. Levi, and Z. Yin, (2021), arXiv:2112.01509 [hep-th].
 - [30] S. Foffa, R. Sturani, and W. J. Torres Bobadilla, *JHEP* **02**, 165 (2021), arXiv:2010.13730 [gr-qc].
 - [31] R. A. Porto, *Phys. Rev. D* **73**, 104031 (2006), arXiv:gr-qc/0511061.
 - [32] R. A. Porto and I. Z. Rothstein, *Phys. Rev. Lett.* **97**, 021101 (2006), arXiv:gr-qc/0604099.
 - [33] R. A. Porto and I. Z. Rothstein, *Phys. Rev. D* **78**, 044013 (2008), [Erratum: *Phys.Rev.D* 81, 029905 (2010)], arXiv:0804.0260 [gr-qc].
 - [34] R. A. Porto and I. Z. Rothstein, *Phys. Rev. D* **78**, 044012 (2008), [Erratum: *Phys.Rev.D* 81, 029904 (2010)], arXiv:0802.0720 [gr-qc].
 - [35] B. Kol and M. Smolkin, *Class. Quant. Grav.* **25**, 145011 (2008), arXiv:0712.4116 [hep-th].
 - [36] J. B. Gilmore and A. Ross, *Phys. Rev. D* **78**, 124021 (2008), arXiv:0810.1328 [gr-qc].
 - [37] M. Levi, *Phys. Rev. D* **82**, 064029 (2010), arXiv:0802.1508 [gr-qc].
 - [38] M. Levi, *Phys. Rev. D* **85**, 064043 (2012), arXiv:1107.4322 [gr-qc].
 - [39] M. Levi and J. Steinhoff, *JCAP* **12**, 003 (2014), arXiv:1408.5762 [gr-qc].
 - [40] M. Levi and J. Steinhoff, *JCAP* **01**, 008 (2016), arXiv:1506.05794 [gr-qc].
 - [41] M. Levi, *Phys. Rev. D* **82**, 104004 (2010), arXiv:1006.4139 [gr-qc].
 - [42] M. Levi and J. Steinhoff, *JCAP* **01**, 011 (2016), arXiv:1506.05056 [gr-qc].
 - [43] M. Levi, A. J. McLeod, and M. Von Hippel, *JHEP* **07**, 115 (2021), arXiv:2003.02827 [hep-th].
 - [44] B. Kol and M. Smolkin, *Phys. Rev. D* **85**, 044029 (2012), arXiv:1009.1876 [hep-th].
 - [45] M. Levi, *Rept. Prog. Phys.* **83**, 075901 (2020), arXiv:1807.01699 [hep-th].
 - [46] M. Levi and J. Steinhoff, *Class. Quant. Grav.* **34**, 244001 (2017), arXiv:1705.06309 [gr-qc].
 - [47] B. R. Holstein and J. F. Donoghue, *Phys. Rev. Lett.* **93**, 201602 (2004), arXiv:hep-th/0405239.
 - [48] V. A. Smirnov, *Springer Tracts Mod. Phys.* **211**, 1 (2004).